Article

Carbon Nanotube-Quenched Fluorescent Oligonucleotides: Probes that Fluoresce upon Hybridization

Ronghua Yang, Jianyu Jin, Yan Chen, Na Shao, Huaizhi Kang, Zeyu Xiao, Zhiwen Tang, Yanrong Wu, Zhi Zhu, and Weihong Tan

J. Am. Chem. Soc., **2008**, 130 (26), 8351-8358 • DOI: 10.1021/ja800604z • Publication Date (Web): 05 June 2008

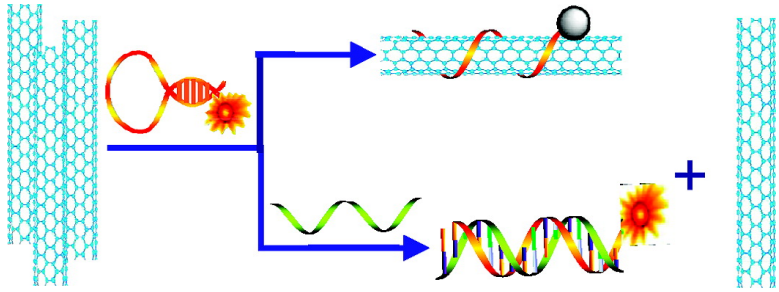

J|A|C|S
ARTICLES

Published on Web 06/05/2008

Carbon Nanotube-Quenched Fluorescent Oligonucleotides: Probes that Fluoresce upon Hybridization

Ronghua Yang,*,†,‡ Jianyu Jin,† Yan Chen,‡ Na Shao,† Huaizhi Kang,‡ Zeyu Xiao,‡ Zhiwen Tang,‡ Yanrong Wu,‡ Zhi Zhu,‡ and Weihong Tan*,‡

Beijing National Laboratory for Molecular Sciences, College of Chemistry and Molecular Engineering, Peking University, Beijing 100871, China, and Center for Research at the Bio/Nano Interface, Department of Chemistry and Department of Physiology and Functional Genomics, Shands Cancer Center, UF Genetics Institute, McKnight Brain Institute, University of Florida, Gainesville, Florida 32611-7200

Received January 24, 2008; E-mail: yangrh@pku.edu.cn; tan@chem.ufl.edu

Abstract: We report an effective, novel self-assembled single-wall carbon nanotube (SWNT) complex with an oligonucleotide and demonstrate its feasibility in recognizing and detecting specific DNA sequences in a single step in a homogeneous solution. The key component of this complex is the hairpin-structured fluorescent oligonucleotide that allows the SWNT to function as both a "nanoscaffold" for the oligonucleotide and a "nanoquencher" of the fluorophore. Given this functionality, this carbon nanotube complex represents a new class of universal fluorescence quenchers that are substantially different from organic quenchers and should therefore have many applications in molecular engineering and biosensor development. Competitive binding of a DNA target and SWNTs with the oligonucleotide results in fluorescence signal increments relative to the fluorescence without a target as well as in marked fluorescence quenching. In contrast to the common loop-and-stem configuration of molecular beacons (MBs), this novel fluorescent oligonucleotide needs only one labeled fluorophore, yet the emission can be measured with little or no background interference. This property greatly improves the signal-to-background ratio compared with those for conventional MBs, while the DNA-binding specificity is still maintained by the MB. To test the interaction mechanisms of the fluorescent oligonucleotide with SWNTs and target DNA, thermodynamic analysis and fluorescence anisotropy measurements, respectively, were applied. Our results show that MB/SWNT probes can be an excellent platform for nucleic acid studies and molecular sensing.

Introduction

The continuous development of fluorogenic probes for molecular interaction studies and ultrasensitive bioanalysis is critically important to medical diagnosis, disease prevention, and drug discovery. This explains the attention given to such well-known DNA hybridization probes as Taqman,[1] protease probes,[2] and molecular beacons (MBs).[3,4] In general, an MB is a dual-labeled oligonucleotide probe with a hairpin-shaped structure in which the 5′ and 3′ ends are self-complementary, bringing a fluorophore and a quencher into close proximity and resulting in fluorescence quenching of the fluorophore.[3] Binding of this probe to a complementary nucleic acid target creates a relatively rigid probe−target hybrid, causing disruption of the hairpin stem and thereby restoring the fluorescence of the fluorophore. The unique thermodynamics and specificity of MBs[5–7] in comparison with linear DNA probes have led to their widespread use in quantitative PCR,[8–11] protein−DNA interaction studies,[12–14] and visualization of RNA expression in living cells.[15–18]

* Corresponding author. Phone: (352) 846-2410 (W.T.).
† Peking University.
‡ University of Florida.

(1) Holland, P. M.; Abramson, R. D.; Watson, R.; Gelfand, D. H. *Proc. Natl. Acad. Sci. U.S.A.* **1991**, *88*, 7276–7280.
(2) Matayoshi, E. D.; Wang, G. T.; Krafft, G. A.; Erickson, J. *Science* **1990**, *247*, 954–958.
(3) Tyagi, S.; Kramer, F. R. *Nat. Biotechnol.* **1996**, *14*, 303–308.
(4) (a) Yang, C. J.; Medley, C. D.; Tan, W. H. *Curr. Pharm. Biotechnol.* **2005**, *6*, 445–452. (b) Marras, S. A. E. *Methods Mol. Biol.* **2006**, *335*, 3–16.
(5) Bonnet, G.; Tyagi, S.; Libchaber, A.; Kramer, F. R. *Proc. Natl. Acad. Sci. U.S.A.* **1999**, *96*, 6171–6176.
(6) Tsourkas, A.; Behlke, M. A.; Rose, S. D.; Bao, G. *Nucleic Acids Res.* **2003**, *31*, 1319–1330.
(7) Bonnet, G.; Krichevsky, O.; Libchaber, A. *Proc. Natl. Acad. Sci. U.S.A.* **1998**, *95*, 8602–8606.
(8) Fang, Y.; Wu, W.-H.; Pepper, J. L.; Larsen, J. L.; Marras, S. A. E; Nelson, E. A.; Epperson, W. B.; Christopher-Hennings, J. *J. Clin. Microbiol.* **2002**, *40*, 287–291.
(9) Poddar, S. K. *Mol. Cell. Probes* **2002**, *14*, 25–32.
(10) Roy, S.; Kabir, M.; Mondal, D.; Ali, I. K.; Petri, W. A., Jr.; Haque, R. *J. Clin. Microbiol.* **2005**, *43*, 2168–2172.
(11) Feldman, S. H.; Bowman, S. G. *Lab Anim. (NY)* **2007**, *36* (9), 43–50.
(12) Li, J. W. J.; Fang, X. H.; Schuster, S. M.; Tan, W. H. *Angew. Chem., Int. Ed.* **2000**, *39*, 1049–1052.
(13) Li, J. W. J.; Fang, X. H.; Tan, W. H. *Biochem. Biophys. Res. Commun.* **2002**, *292*, 31–40.
(14) Orru, G.; Ferrando, M. L.; Meloni, M.; Liciardi, M.; Savini, G.; De Santis, P. *J. Virol. Methods* **2006**, *137*, 34–42.
(15) Fang, X. H.; Mi, Y. M.; Li, J. W. J.; Beck, T.; Schuster, S.; Tan, W. H. *Cell Biochem. Biophys.* **2002**, *37*, 71–81.
(16) Bratu, D. P.; Cha, B. J.; Mhlanga, M. M.; Kramer, F. R.; Tyagi, S. *Proc. Natl. Acad. Sci. U.S.A.* **2003**, *100*, 13308–13313.
(17) Mhlanga, M. M.; Vargas, D. Y.; Fung, C. W.; Kramer, F. R.; Tyagi, S. *Nucleic Acids Res.* **2005**, *33*, 1902–1912.

While MBs have been employed in a broad spectrum of applications, they have also demonstrated significant flaws. For instance, in principle, the fluorophore should be quenched completely by the quencher in the stem-closed form. In reality, however, the residual fluorescence usually varies, which greatly limits detection sensitivity. In addition, MBs are prone to false-positive signals as a result of endogenous nuclease degradation and nonspecific binding by DNA- or RNA-binding proteins. Finally, synthesizing an MB is a complicated task. Specifically, the quality of the synthesis and purification of the probe affect the increment of fluorescence intensity upon hybridization for a given target. Efforts to solve these problems have included the following strategies: introducing novel signaling schemes,[19–22] exploring nanocomposites,[23–25] synthesizing the probe molecules with nuclease-resistant backbones or locked nucleic-acid bases,[26–29] and making better quenchers using rational molecular design coupled with sophisticated synthesis.[30–33] In general, however, effective solutions to the problems enumerated above are limited, and this has driven the search for new methods and materials.

These new types of analytical tools for life science and biotechnology have been created by combining the highly specific recognition ability of biomolecules with the unique structural character of inorganic nanomaterials such as nanocrystals, nanotubes, and nanowires.[34,35] In particulary, carbon nanotubes are molecular wires that have become the leading building blocks for nanomaterials and have shown great potential in electronics, optics, mechanics, and biosensing.[36–39] The interactions of single-wall carbon nanotubes (SWNTs) with biological molecules have been intensively studied in recent years. SWNTs that are covalently or noncovalently attached by nucleic acids[40–42] or proteins[44–46] have been shown to be effective for interaction studies[40] separation of nanotubes,[41] and in applications as biosensors[42–44] and drug transporters.[45]

Single-stranded DNA (ssDNA) has recently been demonstrated to interact noncovalently with SWNTs.[40,41] The ssDNA molecules form stable complexes with individual SWNTs, wrapping around them by means of π-stacking interactions between the nucleotide bases and the SWNT sidewalls. Double-stranded DNA (dsDNA) has also been proposed to interact with SWNTs,[47] but its affinity is significantly weaker than that of ssDNA. This difference in the binding interactions of carbon nanotubes with ssDNA and dsDNA has provided the basis for their use in molecular recognition and detection of DNA.[48–55] Most of these applications have been prompted by changes in electrochemical properties common to SWNTs,[48–53] but a few are based on absorption and near-infrared fluorescence of the carbon nanotubes.[54,55]

Recently, and more relevant to the purpose of this study, scattered examples of noncovalent interactions between SWNTs and organic fluorophores or fluorophore-labeled biomolecules have been reported.[38,56,57] Photophysical studies have found that SWNTs can act collectively as quenchers for the fluorophores.[57]

(18) Santangelo, P.; Nitin, N.; Laconte, L.; Woolums, A.; Bao, G. *J. Virol.* **2006**, *80*, 682–688.
(19) Chen, L. H.; McBranch, D. W.; Wang, H. L.; Helgeson, R.; Wudl, F.; Whitten, D. G. *Proc. Natl. Acad. Sci. U.S.A.* **1999**, *96*, 12287–12292.
(20) Tyagi, S.; Marras, S. A. E.; Kramer, F. R. *Nat. Biotechnol.* **2000**, *18*, 1191–1196.
(21) Du, H.; Disney, M. D.; Miller, B. L.; Krauss, T. D. *J. Am. Chem. Soc.* **2003**, *125*, 4012–4013.
(22) Stoermer, R. L.; Cederquist, K. B.; McFarland, S. K.; Sha, M. Y.; Penn, S. G.; Keating, C. D. *J. Am. Chem. Soc.* **2006**, *128*, 16892–16930.
(23) Dubertret, B.; Calame, M.; Libchaber, A. J. *Nat. Biotechnol.* **2001**, *19*, 365–370.
(24) Seferos, D. S.; Giljohann, D. A.; Hill, H. D.; Prigodich, A. E.; Mirkin, C. A. *J. Am. Chem. Soc.* **2007**, *129*, 15477–15479.
(25) Maxwell, D. J.; Taylor, J. R.; Nie, S. M. *J. Am. Chem. Soc.* **2002**, *124*, 9606–9612.
(26) Braasch, D. A.; Corey, D. R. *Chem. Biol.* **2001**, *8*, 1–7.
(27) Tsourkas, A.; Behlke, M.; Bao, G. *Nucleic Acids Res.* **2002**, *30*, 5168–5174.
(28) Kuhn, H.; Demidov, V. V.; Coull, J. M.; Fiandaca, M. J.; Gildea, B. D.; Frank-Kamenetskii, M. D. *J. Am. Chem. Soc.* **2002**, *124*, 1097–1103.
(29) Wang, L.; Yang, C. J.; Medley, C. D.; Benner, S. A.; Tan, W. H. *J. Am. Chem. Soc.* **2005**, *127*, 15664–15665.
(30) Xia, W.; Whitten, D.; McBranch, D. U.S. Patent 2005030579, 2005.
(31) Cook, R. M.; Lyttle, M.; Dick, D. U.S. Patent 2001-US15082, 2001.
(32) May, J. P.; Brown, L. J.; Rudloff, I.; Brown, T. *Chem. Commun.* **2003**, *8*, 970–971.
(33) Yang, C. J.; Lin, H.; Tan, W. H. *J. Am. Chem. Soc.* **2005**, *127*, 12772–12773.
(34) LaVan, D. A.; Lynn, D. M.; Langer, R. *Nat. Rev. Drug Discovery* **2002**, *1*, 77–84.
(35) Niemeyer, C. M. *Angew. Chem, Int. Ed.* **2001**, *40*, 4128–4158.
(36) Dresselhaus, M. S.; Dresselhaus, G.; Eklund, P. C. *Science of Fullerenes and Carbon Nanotubes*; Academic Press: San Diego, 1996; pp 1−985.
(37) Tasis, D.; Tagmatarchis, N.; Bianco, A.; Prato, M. *Chem. Rev.* **2006**, *106*, 1105–1136.
(38) Britz, D. A.; Khlobystov, A. N. *Chem. Soc. Rev.* **2006**, *35*, 637–659.
(39) Valcárcel, M.; Cárdenas, S.; Simonet, B. M. *Anal. Chem.* **2007**, *79*, 4788–4797.
(40) Zhang, M.; Jagota, A.; Semke, E. D.; Bruce, A.; Diner, B. A.; Mclean, R. S.; Lustig, S. R.; Richardson, R. E.; Tassi, N. G. *Nat. Mater.* **2003**, *2*, 338–342.
(41) Wang, S.; Humphreys, E. S.; Chung, S.-Y.; Delduco, D. F.; Lustig, S. R.; Wang, H.; Parker, K. N.; Rizzo, N. W.; Subramoney, S.; Chiang, Y.-M.; Jagota, A. *Nat. Mater.* **2003**, *2*, 196–199.
(42) Tang, X. W.; Bansaruntip, S.; Nakayama, N.; Yenilmez, E.; Chang, Y. I.; Wang, Q. *Nano Lett.* **2006**, *6*, 1632–1636.
(43) Chen, R. J.; Bangsaruntip, S.; Drouvalakis, K. A.; Kam, N. W. S.; Shim, M.; Li, M. Y.; Kim, W.; Utz, P. J.; Dai, H. J. *Proc. Natl. Acad. Sci. U.S.A.* **2003**, *100*, 4984–4989.
(44) So, H. M.; Won, K.; Kim, Y. H.; Kim, B. K.; Ryu, B. H.; Na, P. S.; Kim, H.; Lee, J. O. *J. Am. Chem. Soc.* **2005**, *127*, 11906–11907.
(45) Shim, M.; Shi Kam, N. W.; Dai, H. J. *J. Am. Chem. Soc.* **2005**, *127*, 6021–6026.
(46) Pantarotto, D.; Partidos, C. D.; Hoebeke, J.; Brown, F.; Kramer, E.; Briand, J. P.; Muller, S.; Prato, M.; Bianco, A. *Chem. Biol.* **2003**, *10*, 961–966.
(47) Franchini, M.; Veneri, D. *Ann. Hematol.* **2005**, *84*, 347–352.
(48) Li, J.; Ng, H. T.; Cassell, A.; Fan, W.; Chen, H.; Ye, Q.; Koehne, J.; Han, J.; Meyyappan, M. *Nano Lett.* **2003**, *3*, 597–602.
(49) Davis, J. J.; Coleman, K. S.; Azamian, B. R.; Bagshaw, C. B.; Green, M. L. H. *Chem.—Eur. J.* **2003**, *9*, 3732–3739.
(50) Wang, J.; Liu, G.; Jan, M. R. *J. Am. Chem. Soc.* **2004**, *126*, 3010–3011.
(51) So, H. M.; Won, K.; Kim, Y. H.; Kim, B. K.; Ryu, B. H.; Na, P. S.; Kim, H.; Lee, J. O. *J. Am. Chem. Soc.* **2005**, *127*, 11906–11907.
(52) Staii, C., Jr. *Nano Lett.* **2005**, *5*, 1774–1778.
(53) Hahm, J.; Lieber, C. *Nano Lett.* **2004**, *4*, 51–54.
(54) Star, A.; Tu, E.; Niemann, J.; Gabriel, J. P.; Joiner, C. S.; Valcke, C. *Proc. Natl. Acad. Sci. U.S.A.* **2006**, *104*, 921–926.
(55) Jeng, E. S.; Moll, A. E.; Roy, A. C.; Gastala, J. B.; Strano, M. S. *Nano Lett.* **2006**, *6*, 371–375.
(56) (a) Li, H. P.; Zhou, B.; Lin, Y.; Gu, L. R.; Wang, W.; Fernando, K. A. S.; Kumar, S.; Allard, L.; Sun, Y. P. *J. Am. Chem. Soc.* **2004**, *126*, 1014–1015. (b) Nakayama-Ratchford, N.; Bangsaruntip, S.; Sun, X. M.; Welsher, K.; Di, H. J. *J. Am. Chem. Soc.* **2007**, *129*, 2448–2449. (c) Boul, P. J.; Cho, D. G.; Rahman, G. M. A.; Marquez, M.; Ou, P. Z.; Kadish, K. M.; Guldi, D. M.; Jonathan, L.; Sessler, J. L. *J. Am. Chem. Soc.* **2007**, *129*, 5683–5687.
(57) (a) Lu, Q.; Freedman, K. O.; Rao, R.; Lee, J.; Larcom, L. L.; Rao, A. M.; Ke, P. C. *J. Appl. Phys.* **2004**, *96*, 6772–6775. (b) Jeng, E. S.; Moll, A. E.; Roy, A. C.; Gastala, J. B.; Strano, M. S. *Nano Lett.* **2006**, *6*, 371–375. (c) Kim, N. W. S.; O′Connell, M.; Wisdom, J. A.; Dai, H. J. *Proc. Natl. Acad. Sci. U.S.A.* **2005**, *102*, 11600–11605. (e) Lin, S. J.; Keskar, G.; Wu, Y. N.; Wang, X.; Mount, A. S.; Klaine, S. J.; Moore, J. M.; Rao, A. M.; Ke, P. C. *Appl. Phys. Lett.* **2006**, *89*, 143118.

Table 1. Designs of Probes and Target Oligonucleotides

type	sequence
FAM-labeled MB (**1**)[a]	5′-Dabcyl-CCTAGCTCTAAATCAC TATGGTCGCGCTAGG-FAM-3′
FAM-labeled HP (**2**)[b]	5′-CCTAGCTCTAAATCAC TATGGTCGCGCTAGG-FAM-3′
FAM-labeled LN (**3**)[c]	5′-CCTAGCTCTAAATCAC TATGGTCGCCGATCC-FAM-3′
pc-ssDNA (**4**)[d]	5′-GCGACCATAGTGATTTAGA-3′
sm-ssDNA (**5**)[e]	5′-GCGACCATACTGATTTAGA-3′

[a] Molecular beacon. [b] Hairpin-structured probe. [c] Linear probe. [d] Perfectly complementary target. [e] Single-base-mismatched target.

Both energy-transfer and electron-transfer processes are considered to be major deactivation pathways for excited fluorophores on nanotube surfaces. While these results provide strong evidence that such quenching approaches might provide a basis for fluorescence sensing, we are unaware of any studies which have examined SWNTs from the perspective of fluorescence restoration.[37,39] In this work, therefore, we explored the use of a self-assembled quenched complex of fluorescent ssDNA and SWNTs as an efficient MB that can fluorescently detect single-nucleotide variations in DNA in homogeneous solution. The key features of this design are as follows. First, as noted above, ssDNA molecules wrap around individual SWNTs by means of π-stacking interactions between the nucleotide bases and the SWNT sidewalls. Next, because the SWNTs act as both a "nanoscaffold" for the ssDNA and a "nanoquencher" of the fluorophore, only one end of the ssDNA must be labeled with a fluorophore. Under these conditions, the ssDNA molecules self-organize on the surface of the carbon nanotubes, completely quenching the fluorophore. Finally, in the presence of a target, competitive binding of the target and the carbon nanotubes with the ssDNA suppresses the fluorescence quenching, allowing fluorescence-signal enhancement that is large relative to that without a target. This combination of properties results in fluorescence enhancement that is sensitive and specific to the perfectly complementary ssDNA. Furthermore, our novel design, which is based on a simple, cost-effective synthesis, was shown to have a large signal-to-background ratio, high thermostability, and exceptional DNA-binding selectivity. Therefore, from the standpoints of design and engineering, production, and overall function, self-assembled ssDNA−SWNT complexes such as the one studied here can easily replace conventional MBs.

Experimental Section

General Procedures. All of the DNA synthesis reagents were purchased from Glen Research. All of the DNA sequences were synthesized using an ABI3400 DNA/RNA synthesizer. Fluorescein CPG was used for the synthesis of fluorescent oligonucleotides. Fluorescence measurements were performed using a Hitachi F-4500 fluorescence spectrofluorometer. Fluorescence anisotropy measurements were conducted using a Fluorolog-3 model FL3−22 spectrofluorometer (HORIBA Jobin Yvon, Edison, NJ) with a 200 μL quartz cuvette. Transmission electron microscopy (TEM) was performed using a transmission microscope (Hitachi H-700). Samples for TEM analysis were prepared by pipetting 5−25 μL of the colloidal solutions onto standard holey carbon-coated copper grids. The grids were dried in air for >12 h before they were loaded into the vacuum chamber of the electron microscope. The TEM samples were not subjected to heavy-metal staining or other treatments.

Choice of Probe and Target DNA. In this work, a hairpin-structured (HP) oligonucleotide containing a 19-base loop and a 6-mer stem was chosen as the recognition element (Table 1). The MB **1** was designed by attaching fluorescein (FAM) and 4-(4′-(dimethylamino)phenylazo)benzoic acid (Dabcyl)[58] to the 3′ and 5′ ends, respectively, of the ssDNA strand. To examine the effect of SWNTs on the fluorescence quenching, the ssDNA was labeled only with FAM at the 3′ end in the HP probe **2**. The target ssDNA molecules **4** and **5** were 19 bases long; **4** was perfectly complementary (pc) to the bases in the loop, while **5** contained a single-base mismatch (sm) with the loop.

Probe **3**, a linear (LN) oligonucleotide labeled with FAM at the 3′ end, was also designed in order to examine the effect of the hairpin structure on fluorescence quenching and target-binding selectivity. As shown in Table 1, this oligonucleotide was 31 bases long, and the 19 bases in the middle of the strand were identical to the 19 bases in the loop of the HP probes. However, it did not have the complementary stem-forming bases on either end and thus could not form a hairpin structure.

Fluorescence-Quenching and Hybridization Assays. The working solution containing the fluorescent oligonucleotide was obtained by dilution of the stock solution to a concentration of 50 nM using phosphate-buffered saline (137 mM NaCl, 2.5 mM Mg^{2+}, 10 mM Na_2HPO_4, and 2.0 mM KH_2PO_4, pH 7.4). The as-grown SWNTs, purchased from Carbon Nanotechnologies, Inc., were sonicated in DMF for 5 h to give a homogeneous black solution. An aliquot of the SWNT suspension [< 3% (v/v)] was added to a phosphate buffer containing the fluorescent oligonucleotide and allowed to incubate for 5−10 min. A 6-fold molar excess of complementary target **4** was then added to the nanotube−conjugate mixture. After this mixture was allowed to hybridize for ~3 h at room temperature, the upper 70% of the clear solution was received. The pellet, which contained impurities, aggregates, and undispersed SWNTs, was removed by ultracentrifugation, and the supernatant was collected. The control solution without target was obtained by addition of the same volume of water to the nanotube complex solution. The solubilized SWNTs by the ssDNA strands were mostly individual tubes and small bundles as revealed by transmission electron microscopy.[59] In order to compare the molecular recognition ability of the nanotube-quenched complex with that of the conventional MB, similar titrations were done with the MB which had Dabcyl as the quencher.

Kinetics and Thermal Profiles. To study the kinetics and time dependence of the fluorescence quenching of the fluorescent oligonucleotides by the carbon nanotubes, fluorescence spectra of solutions containing **2** and SWNTs in the absence or presence of **4** were acquired at time intervals of 20 min, and their peak intensities at 520 nm were plotted as a function of time. For thermodynamic and temperature-dependent studies, the fluorescence of solutions containing **2** and SWNTs in the presence or absence of **4** was measured as a function of temperature.

Results and Discussion

Fluorescence Quenching and Hybridization Assay. Earlier studies have shown that a fluorophore bound to the surface of carbon nanotubes is in fact quenched by them.[38,56] Therefore, when a fluorophore is covalently linked to a biomolecule, the strong binding affinity of the biomolecule for carbon nanotubes is expected to offer a better means of producing highly efficient quenching of the fluorophore.[57] To confirm these findings to our satisfaction, we tested three different nucleic-acid detection methods, based on (i) the conventional MB **1**, (ii) the self-assembled carbon-nanotube complex of **2** (**2**−SWNT), and (iii) the self-assembled carbon-nanotube complex of **3** (**3**−SWNT). We obtained enhancements of the fluorescence emission of **1**−**3** generated by the target DNA in the absence and the presence of SWNTs and evaluated the results in terms of the signal-to-

(58) Marras, S. A. E.; Kramer, F. R.; Tyagi, S. *Nucleic Acids Res.* **2002**, *30*, e122.
(59) See the Supporting Information.

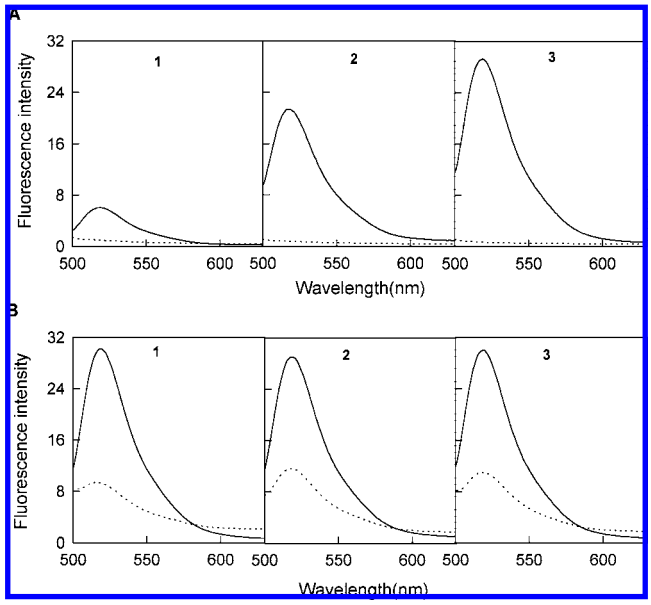

Figure 1. Changes in the fluorescence emissions of **1**−**3** in the phosphate buffer caused by carbon nanotubes and/or the pc-ssDNA target **4**. (A) Fluorescence emission spectra of solutions of **1**, **2**, and **3** in the absence (solid lines) and presence (dotted lines) of SWNTs. (B) Fluorescence emission spectra of solutions **1**, **2**, and **3** containing a 6-fold excess of **4** in the absence (solid lines) and the presence (dotted lines) of SWNTs. The concentrations of **1**−**3** were 50 nM, and the excitation wavelength was 480 nm.

background ratio (S/B), defined as S/B = $(F_{hybrid} - F_{buffer})/(F_{probe} - F_{buffer})$, where F_{probe}, F_{buffer}, and F_{hybrid} are the fluorescence intensities of the probe without target, the plain buffer solution, and the probe−target hybrid, respectively.

In the absence of a target, the background fluorescence signals of **1**−**3** in the phosphate buffer were first studied (Figure 1A). As expected, the background fluorescence observed from **1** was weakest as a result of the formation of hairpin structure, which brings the fluorophore and the quencher into close proximity. For the other fluorescent oligonucleotides, the background fluorescence from **2** was weaker than that from the ssDNA **3**, perhaps as a result of quenching of the FAM fluorescence by the nearby guanine bases in **2**.[60,61] The dotted lines in Figure 1A show the fluorescence emission spectra of **1**−**3** in the presence of SWNTs. Upon excitation at the maximal absorption wavelength of FAM, all of the self-assembled nanotube complexes exhibited decreases in fluorescence intensity relative to that observed for the free fluorescent oligonucleotides under the same conditions. Interestingly, we noted that further fluorescence quenching by the SWNTs was observed even for the MB **1**, indicating that the FAM fluorescence in the hairpin structure was not completely quenched by Dabcyl. In a recent study of noncovalent interactions of SWNTs with fluorescein derivatives,[56b] 67% quenching by SWNTs was observed. However, in our experiment, more than 98% quenching was observed for concentrations of **2** ranging from 50 to 200 nM. The phenomena observed here provide evidence for tight binding of ssDNA on SWNTs.

Specifically, the present nanotube-quenching approaches were found to be highly efficient in probing biomolecular interactions. Figure 1B shows the fluorescence emission spectra of free **1**−**3**

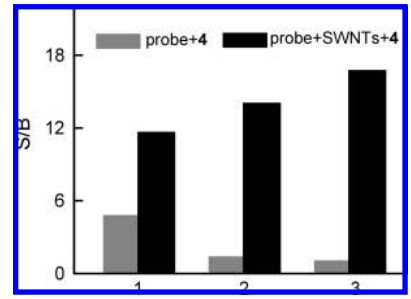

Figure 2. Comparisons of the signal-to-background ratio (S/B) of the fluorescent oligonucleotides generated by a 6-fold excess of the pc-ssDNA target **4** in the absence (gray bars) and presence (black bars) of SWNTs. The concentrations of **1**−**3** were 50 nM, and the excitation and emission wavelengths were 480 and 520 nm, respectively.

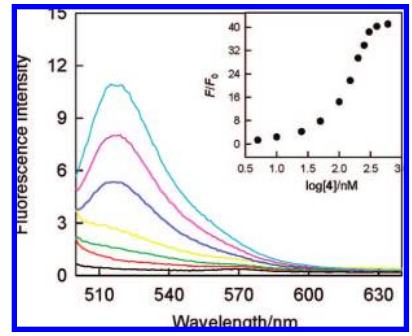

Figure 3. Fluorescence emission spectra of **2**−SWNT (50 nM, $\lambda_{ex} = 480$ nm) in the presence of different concentrations of **4**. Inset: the fluorescence intensity ratio F/F_0 (where F_0 and F are the fluorescence intensities of **2**−SWNT in the absence and presence, respectively, of **4**) plotted against the logarithm of the concentration of **4**.

and their self-assembled SWNT complexes in the presence of the pc-ssDNA target **4**. Competitive hybridization of **4** and SWNTs with the fluorescent oligonucleotide suppresses fluorescence quenching of FAM, whose fluorescence was enhanced in comparison with that in the absence of target. There was a rather large variation in S/B in these assays because of the different background signals of the probes. The experimental results are summarized in Figure 2. In the absence of carbon nanotubes, the fluorescence intensity of **1** was increased by addition of **4**, but for the other fluorescent oligonucleotides, such enhancements of fluorescence intensity were not obvious. The S/Bs generated by the 6-fold excess of **4** were 5.6, 1.4, and 1.1 for **1**, **2**, and **3**, respectively. The stronger background fluorescences from **2** and **3** led to smaller S/Bs compared with the results of the MB assay. In contrast, the presence of SWNTs greatly reduced the background signals for all of the fluorescent oligonucleotides and thus led to large S/Bs. For example, the S/Bs for **1**−**3** generated by the 6-fold excess of **4** in the presence of SWNTs were 13.7, 15.4, and 16.2, respectively, which is a significant improvement compared to the S/Bs in the absence of SWNTs. This comparison clearly demonstrates that the carbon nanotubes greatly improved the S/Bs and, consequently, the analytical sensitivities of the fluorogenic molecular probes. Figure 3 shows the typical fluorescence emission response of **2**−SWNT to increasing concentrations of **4**. A dramatic increase in the FAM fluorescence intensity was observed as the DNA concentration increased from 15.0 to 750 nM. The detection limit (taken to be 3 times the standard deviation in the blank solution) was 4.0 nM, which is 8-fold lower than that of **1**. Moreover, we observed that reducing the concentration of the DNA probe resulted in a lower detection limit. These results

(60) Kurata, S.; Kanagawa, T.; Yamada, K.; Torimura, M.; Yokomaku, T.; Kamagata, Y.; Kurane, R. *Nucleic Acids Res.* **2001**, *29*, e34.
(61) Dohno, C.; Saito, I. *ChemBioChem* **2005**, *6*, 1075–1081.

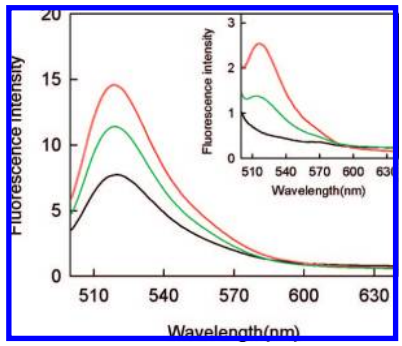

Figure 4. Fluorescence spectra in the presence of the pc-ssDNA target **4** (red curves), the sm-ssDNA target **5** (green curves), and no target (black curves), demonstrating the abilities of **1** and **2**−SWNT (inset) to distinguish perfectly complementary and single-base-mismatched DNA targets. The concentrations of **1** and **2** were 50 nM, and the target concentrations were 100 nM. The excitation wavelength was 480 nm.

suggest that the proposed approach is potentially appropriate for quantification of nucleic acid content in physiological fields. Several reported MB sequences were synthesized without quencher. This significantly improved the S/B compared to values reported for the regular MBs, demonstrating that the present approach provides a universal fluorescent probe for bioanalysis.

The quenching efficiencies of self-assembled nanotube complexes and gold nanoparticles were also compared. Because of their exceptional quenching capabilities, gold nanoparticles have been successfully used to construct fluorescent probes.[23–25] In the classic work of Dubertret's group, for example, single-base-mismatch detection and efficient quenching (up to 99.96% under favorable conditions) were achieved by replacement of Dabcyl with 1.4-nm gold clusters (nanogold) in the MB.[23] However, their nanogold clusters are too small to develop surface plasmon resonances, and the gold−DNA linkage is unstable under the temperature cycling conditions of PCR. Moreover, the tedious processes involved in preparation of the nanoparticles and covalent labeling of the DNA with the nanoparticles hinder the application of gold clusters as a common approach for bioanalysis. While the present self-assembled SWNT complex has high quenching efficiency and single-base-mismatch detection ability equal to gold nanoparticles (see below), our design offers additional advantages, including simplicity of preparation and manipulation as well as greater stability.

DNA Detection Specificity. A significant advantage of MBs stems from the high degree of specificity with which they can recognize target sequences.[3,23] Notwithstanding this performance, the self-assembled nanotube complex shows the same ability to discriminate between the perfect target and the mismatched one, thus outperforming MBs. This assessment is based on the basic competition between unimolecular hairpin formation and bimolecular probe−target hybridization. Our results showed that addition of a low concentration of a noncomplementary DNA had little effect on the fluorescence of either **1** or **2**−SWNT, confirming the high specificity of the hairpin structure. However, a high concentration of the noncomplementary DNA results in a large background signal for **2**−SWNT due to competitive binding of the DNA and **2** with the carbon nanotubes. The pc-ssDNA target **4** and the sm-ssDNA target **5** were then used to compare the DNA detection specificities of **1** and **2**−SWNT. Figure 4 displays fluorescence emission spectra of **1** (50 nm) in the presence of **4** or **5** (100 nm). Both targets increased the fluorescence emission of **1**, and the fluorescence enhancement by the sm target **5** was 82% of that by the pc target **4**. For **2**−SWNT (Figure 4 inset), the enhancement by **5** was only 64% of that by **4**. These results reveal that the ability of **2**−SWNT to detect a single-base mismatch is slightly greater than that of **1**.

To illustrate the DNA binding specificity more clearly, we introduced a selectivity coefficient, α, defined as $\alpha = (S/B)_{i\cdot j}/(S/B)_{i\cdot j'}$, where $(S/B)_{i\cdot j}$ is the S/B value for the DNA probe i in the presence of DNA target j and $(S/B)_{i\cdot j'}$ is that for the same DNA probe in the presence of target j′. The selectivity of each probe for the pc-DNA target **4** was used as the standard ($\alpha = 1$). A selectivity coefficient of 0.764 of **1** for **5** over **4** was obtained, while the analogous selectivity coefficient of **2**−SWNT for **5** over **4** was $\alpha = 0.472$. These selectivity coefficients show that the sm-recognition ability of a hairpin-DNA probe can be improved using carbon nanotubes. To further characterize the binding specificity of **2**−SWNT for **4**, the competitive complex was also analyzed in the presence of biologically related substrates. The addition of **4** to a mixture containing **2**−SWNT and DNA (100 nM), protein (bovine serum albumin, 1.0 μg/mL), and amino acids [histidine, cysteine, glutamic acid, and aspartic acid (each 10 μM)] gave fluorescence response curves almost superimposable on the one obtained exclusively in presence of **4**,[59] although the background signal displayed a small increase in the mixture. These results clearly indicate that **2**−SWNT is not sensitive to other targets.

The probe containing the linear DNA strand further illustrates the importance of the relationship between carbon nanotubes and selectivity. The selectivity coefficient of **3**−SWNT for **5** over **4** was 0.833, which is slightly smaller than that of MBs; however, it is higher than the coefficient of linear DNA probes that cannot discriminate sm targets. The contrasting results clearly demonstrate that the carbon nanotubes are promising building blocks for DNA binding specificity. To account for this outcome, we reasoned that the oligonucleotide is initially bound to the nanotube and that the target DNA must then compete with the nanotube for the bound oligonucleotide. Under these conditions, only the perfectly complementary DNA, rather than the mismatched DNA, could displace the nanotube from the assembled complex and form the DNA−DNA hybridization product.

Kinetics and Thermodynamics. The kinetic and thermodynamic properties of carbon-nanotube binding and subsequent DNA hybridization of the fluorescent oligonucleotides are fundamentally different from those of conventional MBs. Adsorption of ssDNA on the carbon nanotube surface is slow at room temperature. Figure 5 shows fluorescence quenching of **2** by SWNTs in the phosphate buffer as a function of time. The curve exhibits a rapid reduction of fluorescence intensity in the first hour followed by a slower decrease over the next 2−3 h. We believe that the surface effect of the carbon nanotubes and the charge properties of the ssDNA may be the main contributors to the small adsorption rate. In the presence of **4**, competitive binding of **4** and SWNTs with **2** reduces adsorption of **2** on the nanotube surface, which hinders fluorescence quenching. However, DNA hybridization in the presence of SWNTs is also slower than free DNA hybridization without carbon nanotubes at room temperature. The best S/B was obtained at 3 h, when the DNA−SWNT complexes had reacted with their target DNA (Figure 4 inset).

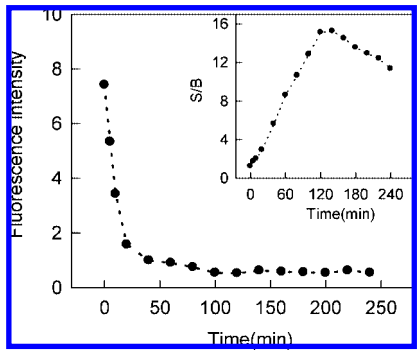

Figure 5. Fluorescence quenching of **2** by SWNTs in the phosphate buffer as a function of time. Inset: a plot of the S/B of **2**−SWNT generated by a 6-fold excess of target **4** as a function of time. The concentration of **2** was 50 nM, and the excitation and emission wavelengths were 480 and 520 nm, respectively.

Shorter or longer interaction times produced probes with correspondingly smaller S/Bs. An understanding of this phenomenon may be gained by a comparison of the slow hybridization of DNA−SWNT complexes with the slow binding observed for MBs with long stems. In the case of MBs, the reduced binding rate is normally accompanied by an increase in target binding specificity. For carbon nanotubes, strong adsorption of the ssDNA to the nanotube surface results in the formation of a barrier against nanotube replacement, which affects hybridization because the DNA probe is on the nanotube surface. Nevertheless, it is possible that the rates of both nanotube binding and DNA hybridization could be accelerated by sonication. When the solution was allowed to stand for 5 min at room temperature, 30% of the fluorescence of **2** was quenched by SWNTs, but nearly 80% fluorescence quenching was observed under the same conditions upon continuous sonication for 5 min. The corresponding S/Bs in the presence of a 6-fold excess of **4** were 3.1 and 4.8, respectively.

Melting-temperature measurements were then conducted to study the thermostability of the SWNT complex. We first monitored the fluorescence of **1** incubated at different temperatures. The results showed that at lower temperatures, the MB is in a closed state and weakly fluoresces. However, at high temperatures, the helical order of the stem gives way to a random-coil configuration, separating the fluorophore from the quencher and restoring a higher degree of fluorescence (Figure 6, trace a). This experiment was repeated using **2**−SWNT. After **2** and SWNTs were mixed at room temperature for 3 h, the mixture was exposed to different temperatures between 10 and 85 °C in 5 °C increments. We found that the nanotube complex displays excellent thermostability even at high temperatures, as indicated by the minimal changes in fluorescence intensity at temperatures above 60 °C (Figure 6, trace b). This unusual behavior suggests that the nanotube surface with adsorbed ssDNA strands is much less dependent on temperature than a conventional MB, where DNA is observed to melt. This implies that exceptionally strong affinity between ssDNA and carbon nanotubes exists. Such tight binding between the nanotube and ssDNA strands makes **2**−SWNT function well at both room temperature and relatively high temperatures. Figure 7 compares the S/Bs after hybridization of both **1** and **2**−SWNT with **4** at 25 and 75 °C, respectively. **2**−SWNT hybridized to its target at 75 °C had an S/B of 7.8, which is significantly higher than the S/B of 1.2 observed for

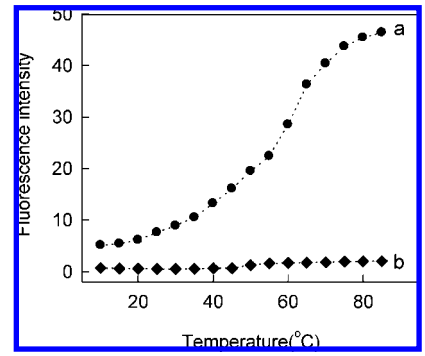

Figure 6. Temperature effects on the fluorescence emission intensities of (a) **1** and (b) **2**−SWNT. Fluorescence measurements on **2**−SWNT were performed after incubation of **2** and SWNTs for 3 h. The concentrations of **1** and **2** were 50 nM, and the excitation and emission wavelengths were 480 and 520 nm, respectively.

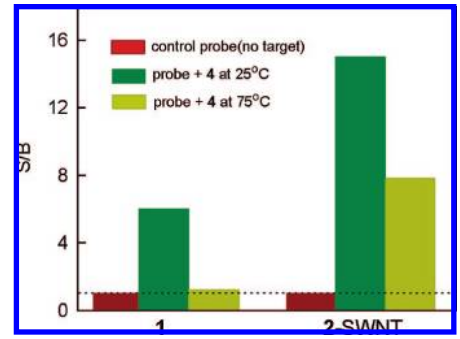

Figure 7. Signal enhancement of both **1** and **2**−SWNT in the phosphate buffer after hybridization with the target **4** at 25 and 75 °C. The final probe/target concentration ratio was 1:6. The excitation and emission wavelengths were 480 and 520 nm, respectively.

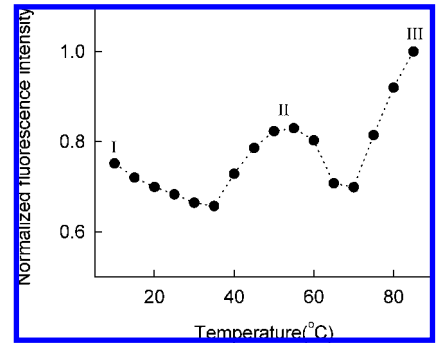

Figure 8. Temperature dependence of the fluorescence intensity (normalized to the highest intensity observed) of **1** in the presence of SWNTs. The temperature was increased from 10 to 85 °C in increments of 5 °C. The excitation and emission wavelengths were 480 and 520 nm, respectively.

hybridized **1** at this temperature. The reduction in the S/B of **2**−SWNT at 75 °C compared with its S/B at 25 °C is due to the decrease of fluorescence intensity of the DNA hybrids at the higher temperature (see below). The thermostability of **2**−SWNT also allows its use in real-time PCR studies under normal temperature-cycling conditions.

Interaction Mechanisms. The experimental data show that the proposed approach works well for assays of biomolecular interaction. However, before our self-assembled SWNT complex can be practically applied as a nanosensor, some questions must be addressed. The first asks whether configuration of the hairpin-structured fluorescent oligonucleotide is changed by the carbon nanotube. The HP ssDNA strand might retain its primary hairpin

Scheme 1. Schematic Representation of the Phase Transitions in Solutions Containing MBs and SWNTs[a]

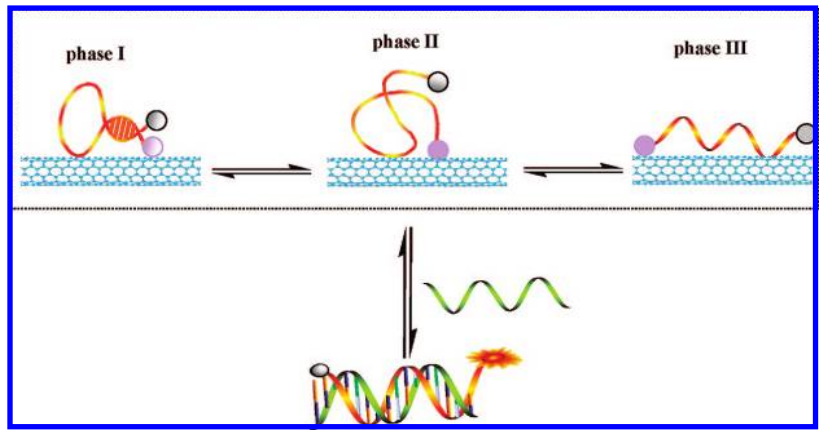

[a] The drawing of fluorophore-functionalized DNA adsorbed on the SWNT is only a graphic presentation and does not represent the precise way that DNA binds on SWNTs.

shape when adsorbed on the SWNTs surfaces. In that case, only some of the DNA segments would interact with SWNTs while other segments would not. Some of the DNA segments could even protrude out into the solution. It is also possible that the HP DNA strand could unfold into a linear DNA strand and completely wrap around a SWNT, thus strongly interacting with the sidewalls of the SWNT. In contrast to the former case, the efficiency of fluorophore quenching by SWNTs in the latter case should be higher.

The fluorescence quenching efficiencies F_0/F, where F_0 and F are the fluorescence intensities of the probe in the absence and presence, respectively, of SWNTs, were obtained for **2** and **3** as functions of time.[59] Compared with **2**, the linear oligonuclotide **3** displays slightly more rapid kinetic quenching behavior as well as a higher quenching efficiency by carbon nanotubes. This result indicates that binding of **3** with carbon nanotubes at room temperature is easier and tighter than that of **2**, implying that the hairpin structure of **2** is probably retained in the presence of carbon nanotubes. To further understand the change in configuration of the hairpin structure adsorbed on the nanotube surface, the effects of temperature on the fluorescences of **1** and **3** in the presence of SWNTs were studied. As the temperature increased, the fluorescence intensity of **3** continuously decreased: for example, the fluorescence intensity of **3** at 85 °C was ~15% of that at 10 °C. This thermodynamic behavior apparently indicates that in the case of **3**−SWNT, the DNA strand exists with only one conformation. On the other hand, the effect of temperature on the fluorescence of **1**−SWNT is more complicated (Figure 8). At low temperatures (<40 °C), the fluorescence intensity decreased slightly as the temperature increased; this behavior was followed by an increase in fluorescence as the temperatures rose to ~60 °C. When the temperature was higher than 60 °C, a second thermodynamic cycle could be observed in which the fluorescence intensity first decreased and then increased with increasing temperature.

This thermodynamic behavior can be interpreted in terms of configuration changes of **1,** as shown in Scheme 1. Specifically, at low temperatures, **1** spontaneously forms a hairpin structure and adsorbs on the carbon nanotube surface. The extent of adsorption increases with increasing temperature, resulting in stronger fluorescence quenching (Scheme 1, phase I). Since the hairpin stem is not sufficiently stable at higher temperatures, the closed MB begins to melt into a random-coil configuration when the temperature is higher than 30 °C (Scheme 1, phase II). This configuration change results in only minimal enhancement of the fluorescence compared with that of the closed form. The MB **1** used in our experiment melts at ~53 °C. In phase II, the fluorescence intensity decreased with a rise in temperature. Since carbon nanotubes favor adsorption of ssDNA as opposed to dsDNA, further increases in temperature may convert the random-coil configuration of **1** into a linear ssDNA, which would completely separate FAM from Dabcyl (Scheme 1, phase III), again leading to fluorescence enhancement. This transition occurred at 65 °C.

Another key question that arises is precisely how the self-assembled nanotube complex interacts with the target in order to produce fluorescence enhancement. The binding interactions of the ssDNA with its target can occur either in solution or at the nanotube surface. In the former case, the ssDNA first leaves the nanotube surface, and then DNA hybridization happens in solution. In the latter case, however, the ssDNA does depart from the nanotube, and target complexation occurs on the nanotube surface. This is where the ssDNA strand undergoes a change in conformation in response to interaction with its target. Therefore, in this case, the dye end of the DNA molecule extends from the SWNT in such a way that it is no longer quenched, while the remaining DNA is still adsorbed to the SWNT.

To understand whether the DNA hybridization occurs on the carbon nanotube surface or in solution, fluorescence anisotropy was used. The fluorescence anisotropy of a fluorophore reflects the molecule's ability to rotate in its microenvironment, which depends on the viscosity of the solution, the fluorescence lifetime of the fluorophore, and the size and mass of the molecule to which the fluorophore is attached.[62] Therefore, fluorescence anisotropy can be used to judge whether the DNA hybridization occurs on the carbon nanotube surface or in solution on the basis of the difference in the molecular weights of the fluorescent oligonucleotides. The fluorescence anisotropy of the free state of **2** in the phosphate buffer was 0.0398 ± 0.012; this value was minimally increased by the addition of a 6-fold excess of **4** but increased ~19-fold by addition of SWNTs,[59] indicating

(62) Lakowicz, J. *Principles of Fluorescence Spectroscopy* 3rd ed.; Springer: New York, 2006.

formation of nanotube complexes. However, when **4** was added to the solution of **2**−SWNT, the fluorescence anisotropy did not increase but instead decreased sharply in comparison to that of **2**−SWNT, yielding a value nearly equal to that for **2** upon addition of **4**. To further confirm that the DNA hybridization occurred in solution, we isolated the hybridized DNA complexes by dialysis against the phosphate buffer using a membrane (molecular weight cutoff 8000−14400) and measured the fluorescence intensity of the dialysis product and the nanotube complex. Specifically, while the nanotube complex inside the membrane was nonfluorescent, we found the product outside the membrane to be highly fluorescent.[59] These fluorescence intensity results combined with the fluorescence anisotropy data demonstrate that DNA hybridization occurs in solution rather than on the nanotube surface.

Conclusion

In summary, we have proposed a novel self-assembled SWNT−oligonucleotide complex and demonstrated its feasibility in the recognition and detection of specific DNA sequences in a single step. The nanotube complex represents a new class of universal fluorescence quenchers that are substantially different from organic quenchers and should therefore find many applications in molecular engineering and biosensor development. Although DNA hybridization of the nanotube-quenched oligonucleotide is slower than that of MBs, the present approach can be engineered in ways that offer unique advantages and capabilities that are not available from conventional molecular systems. First of all, the approach has revealed unique properties for use in engineering molecular probes. For instance, in contrast to regular MBs, only one end of the DNA strand must be dye-labeled, leading to less laborious and more cost-effective synthesis. Nevertheless, this probe has better sensitivity and higher thermal stability. High thermostability combined with the excellent affinity for a complementary sequence makes this nanotube-complex probe especially useful under stringent experimental conditions. Second, the fluorescence quenching scheme utilized in SWNT-complex probes can also be applied to different types of fluorophores. Finally, this approach can be extended to develop a variety of fluorescent biological probes by designing different DNA strands. We envision that the methods and principles presented here could open up new opportunities for the design and engineering of nanodevices for sensor applications. Moreover, our studies involving nanotube-quenched fluorescent oligonucleotides will certainly provide insights into improving the performance of MBs, which are now widely used in many areas of research. Currently, intensive research on the use of these probes for in vivo monitoring of nucleic acids is being conducted in our laboratory, and the results will be reported in due course.

Acknowledgment. We acknowledge financial support through grants from NIH, NSF, and the National Natural Science Foundation of China (20525518, 20775005).

Supporting Information Available: Figures showing TEM images, the influence of other substrates on fluorescence response, and fluorescence intensities, anisotropies, and quenching efficiencies under various conditions. This material is available free of charge via the Internet at http://pubs.acs.org.

JA800604Z